LAWRENCE
LIVERMORE
NATIONAL
LABORATORY

LLNL-TR-756199

EXPLORATORY PU(III) OXALATE/PU(IV) OXIDE MORPHOLOGY STUDIES

R. A. Torres, B. W. Chung, P. C. Lan, D. J. Roberts

August 7, 2018

Disclaimer

This work performed under the auspices of the U.S. Department of Energy by Lawrence Livermore National Laboratory under Contract DE-AC52-07NA27344.

Pu Processing Signatures- Engineering Design Factors Final Report
Exploratory Pu(III) Oxalate/Pu(IV) Oxide Morphology Studies
July 2018
LLNL.16.011
PI: Richard A. Torres
Contributors: Brandon W. Chung, Pui C. Lan, David J. Roberts

Executive Summary

Exploratory experiments were performed to see if morphological information (particle-size/habit) about PuO_2 might give useful information about growth conditions for its oxalate precursor. We performed experiments with trivalent Pu and its analogue, trivalent cerium (Ce). Movies of the Ce oxalate experiments showed that solution turbidities can be a useful monitor for the precipitation kinetics. It was clear that when mixing was too slow to keep up with oxalic acid addition, precipitates formed locally, and partially redissolved when oxalic addition was complete. The Ce oxalate and oxide particle-sizes determined in liquid slurries by traditional light-scattering instrumentation agreed in general with those found by SEM imaging. The Ce oxalate size distributions depended on the synthesis conditions, but it was not monotonic in the progression from best- to worst-mixed. Uniformity, as measured by the FWHM (full width at half maximum) of the distributions, varied by a factor of two or more. Because the distributions and FWHMs did not change monotonically as synthesis conditions changed from best- to worst-mixed, the utility of the size distributions for Ce as a diagnostic is doubtful.

SEM images showed Ce oxalates grow as multiple clusters of plates with shared edges. Particles grown under the poorest mixing conditions can show “feathery” edges. More experiments are needed to test whether this might be a useful diagnostic.

Pu information is limited to SEM images; we did not have access to a particle-size analyzer for radioactive Pu. We did not make movies because of the logistical difficulties of shooting in a glovebox. Like Ce particles, Pu-oxalate particles also grow as clusters of plates with shared edges. Sputter-coating the Pu particles with a few tens-of-nanometers thick titanium metal coating helped to reduce charging issues that affected the spatial resolution of the images. The oxalate grown under the best-mixed direct strike conditions, Pu-A, was clearly different from the other three Pu materials. Its packing density was ~2-3 times greater than the other Pu oxalates, and there were a greater number of “large” particles. Pu-A particles also appeared more spherical, although it is possible that this is an artifact of the image resolution. In general, the largest Pu particles were ~3 times smaller than the largest Ce particles grown under the same conditions. This suggests that more homogeneous nucleation sites were created simultaneously for Pu as compared to Ce.

Access to a particle-size analyzer that may be used for quantitating Pu size distributions is recommended for any future work.

Introduction

A common plutonium concentration step in aqueous purification processing is the reduction of dissolved plutonium (Pu) from higher oxidation states to the trivalent state, precipitation of Pu^{3+} with dibasic oxalic acid, HOOCCOOH (abbreviated as H_2Ox hereafter), to form $Pu_2(Ox)_3 \cdot 10H_2O$, collecting the solid by filtration, and the subsequent calcining of the Pu-oxalate to PuO_2. Our desire was to see whether the morphology (particle-size and/or habit) of the PuO_2 might provide information about the synthesis conditions.

The commonly assumed precipitation mechanism when an insoluble substance is crystalized from two soluble reagents is nucleation (the creation of sites from soluble complexes where crystallites can begin to grow) and the growth of crystals from further deposition of the insoluble substance onto the sites. Particle-size distributions depend on the number of small crystallization sites created, which then accrete the rest of the insoluble substance, and whether nucleation continues as crystals grow, creating a wider distribution of particle-sizes. Another recognized process which might affect particle-size distributions is Ostwald ripening, which is the tendency of smaller crystals to redissolve in the mother liquor and reprecipitate onto larger crystals. Therefore, factors which conceivably might affect the particle-sizes of the products are the temperature of precipitation, the relative mixing rates of the solutions, the time delay between the precipitation and the separation of the crystals from the mother liquor, and the order of reagent addition.

Instrumentation available at LLNL for investigating these particles are a traditional light-scattering particle-size analyzer for non-radioactive samples, and secondary electron microscopy (SEM)-imaging of non-radioactive and radioactive particles. Because we wanted to compare the information from particle-size analysis and SEM-imaging, we used cerium (Ce) as an analogue for Pu. (Cerium forms insoluble $Ce_2(Ox)_3 \cdot 10H_2O$, which converts to CeO_2 when calcined.) We used an autotitrator to control the addition rate of oxalic acid to the metal solutions, and the mixing rates (the speed of stirring.) A total of eight oxalate samples were produced- three each by the direct strike process (adding oxalic acid solution to the metal solution), and one each by the reverse strike process (adding metal solution to the oxalic acid solution), for Ce and Pu. We did not investigate the effect of temperature or the time between crystallization and filtration.

Reagents

70% Baker Analyzed® nitric acid; 1 *M* HNO_3

32% Optima® hydrochloric acid; 4 *M* HCl; 0.5 *M* HCl

1 *M* Baker Analyzed® oxalic acid dihydrate in water

0.5 *M* Alfa Aesar® $Ce(NO_3)_3 \cdot 6H_2O$ in 1 *M* HNO_3 (Ce assayed by EDTA titration).

All solutions were filtered through 0.2-micron membrane filters before use.

Experimental- Metal Oxalate/Oxide Production

All experiments were performed at ambient temperature. Metal solutions were 1.0 *M* in the appropriate acid (nitric for Ce or hydrochloric for Pu.) We dissolved high purity Pu with HCl as needed to produce $PuCl_3$ solutions. We used a Mettler T50 autotitrator with a three-bladed stirrer and the buret tip near the bottom edge of the cup to add reagents at controlled rates into a near-cylindrical 100-mL titration cup. We used 5 mmol Ce or 6.7 mmol Pu in 65 mL of solution for the direct strike syntheses. We added ~11 mL or ~15 mL of 1 *M* oxalic acid (a 50 mol% excess) to precipitate the Ce and Pu oxalates, respectively. Conditions (reagent addition rate/stirrer speed) for the direct strike syntheses of Ce and Pu oxalates were identical. The time to add reagent was proportionally longer for the Pu experiments. There was a slight difference in ambient temperature for the Ce (~22ºC) and Pu (~17ºC) experiments, because the glovebox nitrogen atmosphere came from liquid nitrogen blow off.

One sample of each metal oxalate was produced under reverse strike conditions (adding the metal solution to the oxalic acid solution.) We could not use the titrator to control the Pu addition rate for reverse strike conditions, since there was not enough plutonium metal available to make enough stock solution to completely fill the autoburet. In this case, the Pu was added in 1-mL increments with a pipettor with plastic tip until 20 mL of 0.33 *M* Pu in 2 *M* HCl had been added to the oxalate solution. Each increment took ~ 0.25 seconds to dispense; ~5 sec elapsed between each addition.

We continued to stir the metal-oxalate slurries for ~5 minutes after the addition of reagent. We vacuum filtered the precipitates onto 0.2-micron membrane filters and washed them once with ~30 mL water and twice with ~30 mL of methanol. (The initial filtration occurred ~30-40 minutes after the initial reagent addition.) We dried them on the filters overnight with continued suction before transferring the oxalates to glass storage vials. Recoveries based on the oxalate weights after transfer to the collection vials ranged from 87-91% for Ce, and 93-96% for Pu.

Portions of the oxalates were calcined in air in ceramic crucibles to produce the oxides. Ce oxalates were calcined at 450ºC for 2 hours, agitated, and reignited at 500ºC for 2 hours. The crucibles were removed while hot and cooled in a Drierite®/Ascarite® desiccator to avoid moisture or CO_2 absorption. Based on the weight changes measured in the calcination crucibles for the four samples, we found 9.8 $\pm$0.2 waters of hydration per $Ce_2(Ox)_3$ molecule.

Pu oxalates were calcined at 500ºC for 6 hours, cooled overnight, agitated, and reignited for an additional 6 hours at 500ºC. The furnace was in an inert glove box (nitrogen atmosphere) with an air supply to the interior of the furnace. The air supply was turned off when the furnace was off. We assumed the glovebox atmosphere was sufficient to minimize possible moisture/CO_2 absorption. We found 9.4 $\pm$ 0.4 waters of

hydration per $Pu_2(Ox)_3$ molecule. Fundamentally, the measurement of the number of waters of hydration for Pu oxalate was subject to more experimental error than the corresponding Ce oxalate measure. We could not determine weight changes directly in the calcination crucibles, because the furnace glovebox did not have an analytical balance in it. We measured the starting and ending weights in glass storage vials before and after calcining, assuming 100% transfer to and from the crucibles.

Experimental- Solution Conditions

We coarsely determined the dependence of mixing times on stirrer speed by monitoring the acid-base reaction of Xylenol Orange at 600 nm with a Brinkmann fiber optic digital colorimeter. A slightly basic (0.0001 *M* NaOH) magenta solution of Xylenol Orange changed to yellow when acidified with 0.4 mL of 0.1 *M* HCl. The colorimetric probe was placed near the top of the solution. Movies of the mixing at various stirrer speeds show the injection of acid out of the buret tip, and the decrease in absorbance with time. Individual movie frames, along with the movie frame rate, allow for the determination of the mixing time. We show an illustrative sequence of screen grabs from a movie with stirrer speed 10% of maximum below.

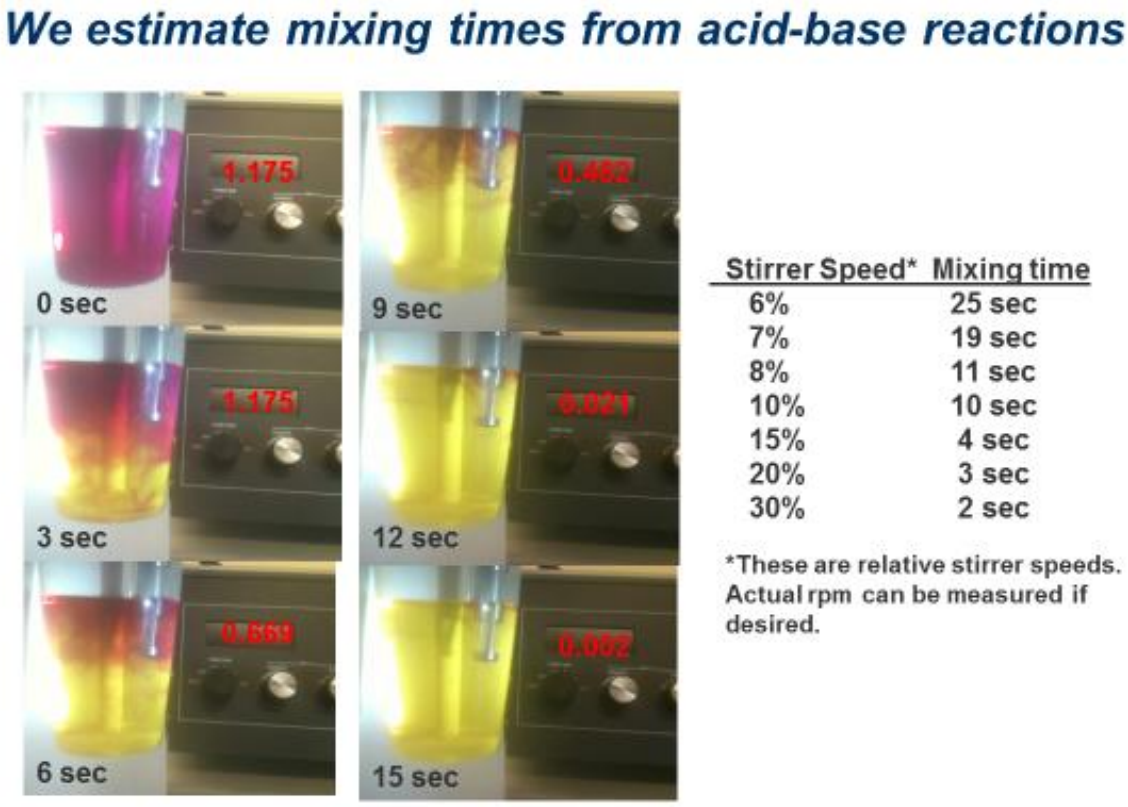

We followed the Ce oxalate precipitation turbidimetrically with the Brinkmann fiber optic probe. As the precipitate forms, it obscures the light returning to the detector, increasing the apparent absorption of the colorless solution. We show an illustrative sequence of screen grabs from a movie with stirrer speed 25% of maximum below.

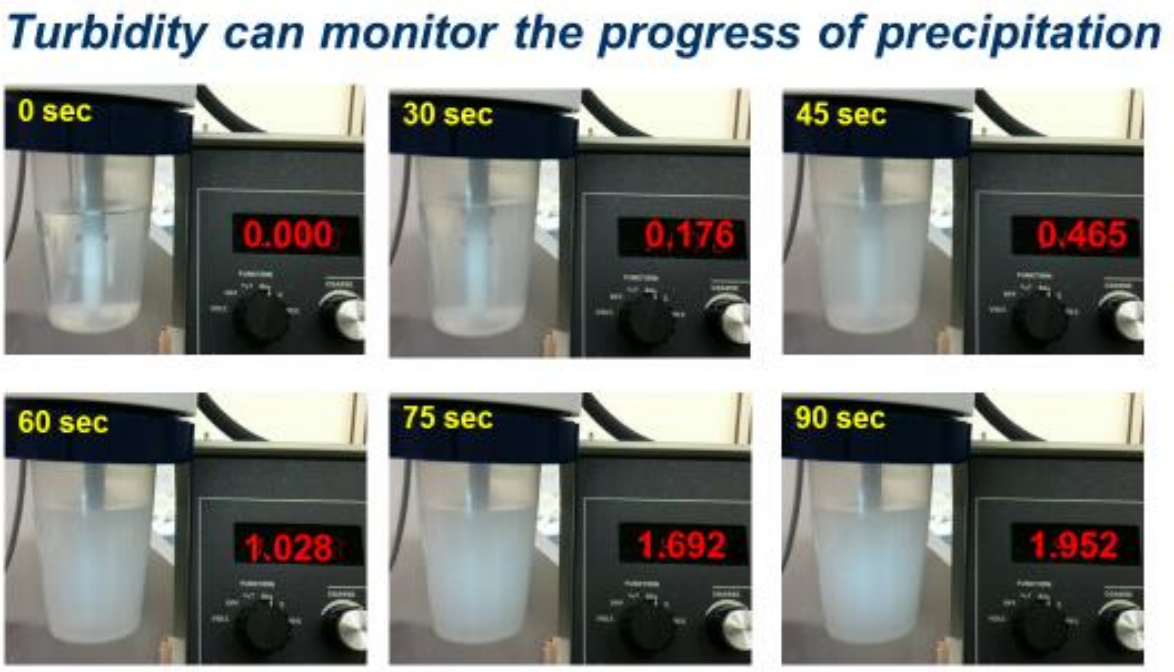

Experimental- Metal Oxalate/Oxide Characterization

We measured Ce oxalate/oxide particle-size distributions with a Micrometrics Instrument Corp. Saturn DigiSizer 5200 in aqueous 35 wt% sucrose. We use the average of three successive scans in our data analysis. The calibration was confirmed with a 5-µm garnet standard.

We acquired Ce SEM images with a JEOL Scanning Electron Microprobe. We did not observe charging issues that affected the spatial resolution of naked Ce particle images. We acquired Pu SEM images with a JEOL Electron Probe Microanalyzer. Naked Pu particles presented significant charging issues that noticeably affected the spatial resolution of the images. We sputter-coated the Pu particles with a few tens-of-nm thick titanium metal layer to reduce the charging difficulties.

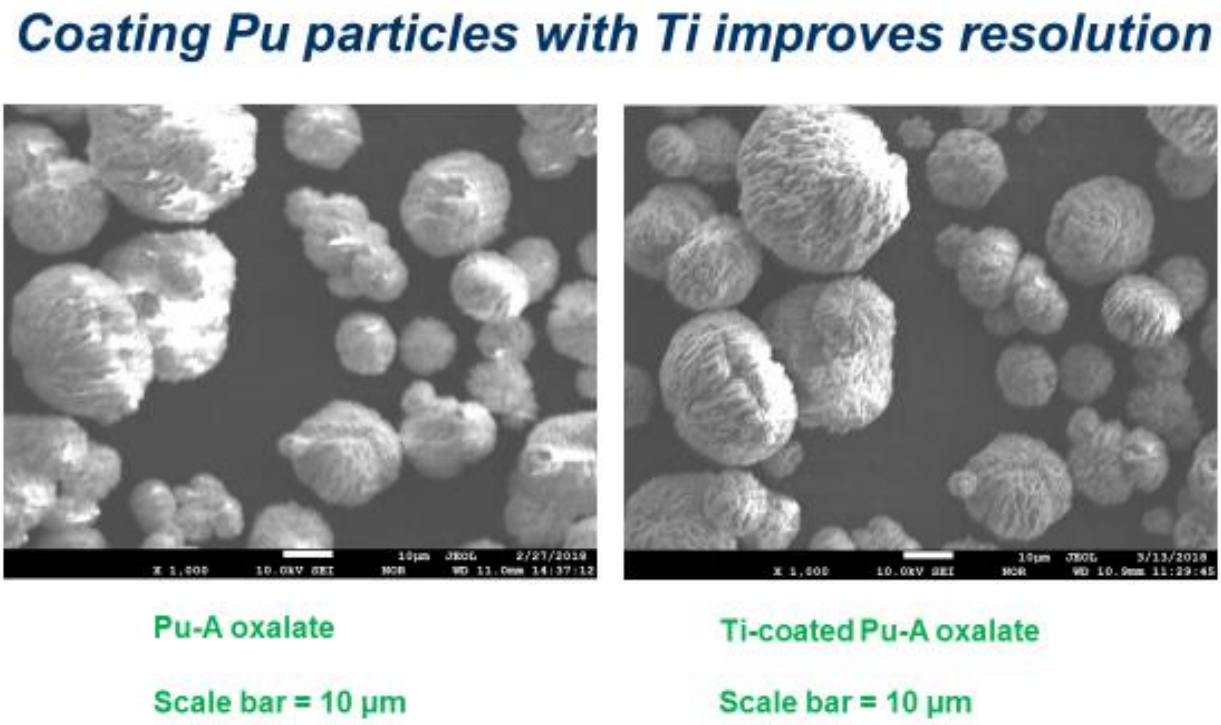

Ce Results and Discussion

Ce oxalate precipitation can be monitored turbidimetrically to obtain kinetic information if desired. The following figure shows there is an induction period before precipitation occurs if the addition of oxalic acid is slow enough compared to the mixing time. When the addition is too fast, the Ce oxalate precipitates rapidly, but redissolves somewhat before continuing. (Note the turbidity spikes at 100% and 150% oxalic acid stoichiometries.) Also, precipitation occurs faster at higher Ce concentration.

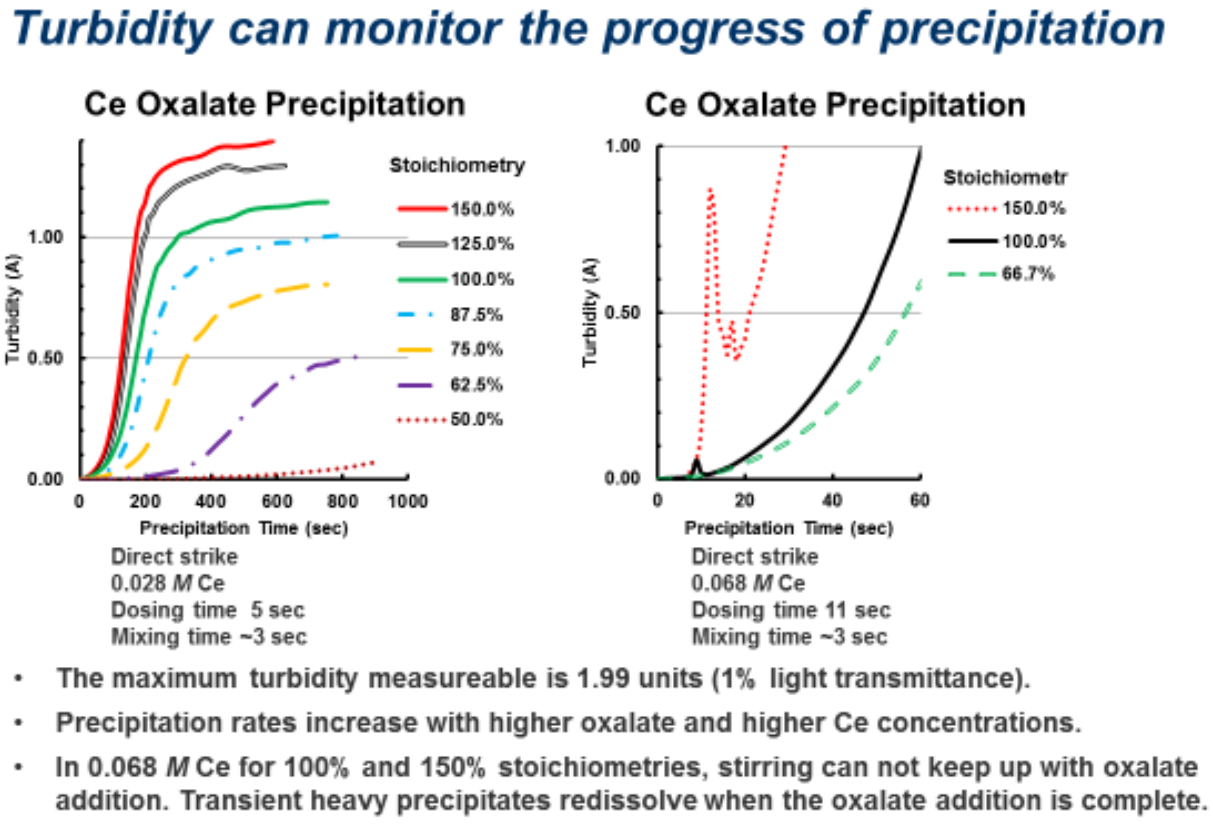

- The maximum turbidity measureable is 1.99 units (1% light transmittance).
- Precipitation rates increase with higher oxalate and higher Ce concentrations.
- In 0.068 *M* Ce for 100% and 150% stoichiometries, stirring can not keep up with oxalate addition. Transient heavy precipitates redissolve when the oxalate addition is complete.

As shown in the following figure, not all of the precipitate is suspended in the slurry if stirring is too slow. Curdy precipitates form initially, which partially redissolve, while simultaneously, more nucleation and homogeneous growth occurs in the poorly mixed supernate. Large agglomerates exist, which are not broken up by the stirrer. These Ce oxalate particles had the largest particle-sizes of all the preparations.

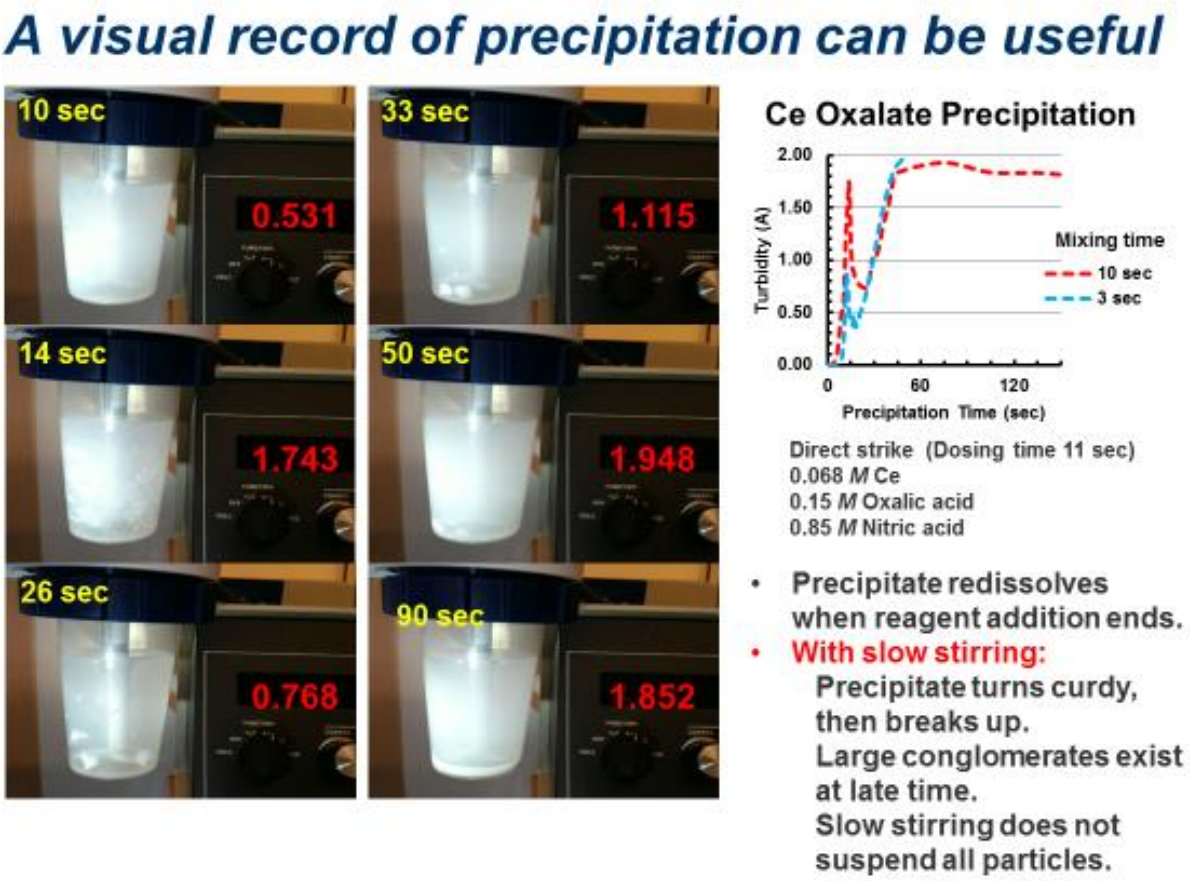

We used 35 wt% aqueous sucrose for traditional light-scattering measurements of particle-sizes. Scans of Ce oxalate typically showed a primary component at less than 150 microns, and a secondary component at 380-480 microns. We believe the larger component is an artifact due to the agglomeration of smaller particles in the slurry. When water was used as the medium (even with surfactant) successive scans showed a monotonic decrease in the intensity of the primary component, with corresponding increases in the secondary component. (Sometimes with water, the secondary component became the dominant one.) With sucrose solution, the secondary component is still evident, but successive scans do not show monotonic changes, and sometimes the secondary component is missing entirely. In addition, the SEM images do not show any particles this large.

Distributions measured for Ce oxalate and oxides are shown below. Of note is that the particle-sizes do not monotonically change as mixing conditions change from best (Ce-A) to worst (Ce-C) for the direct strike syntheses. The best (Ce-A) and worst (Ce-C) mixing conditions give noticeably bigger particles with a broader distribution than the intermediate case (Ce-B). Therefore, it is not likely that the mean particle-size or width of the distribution will be a useful diagnostic.

The oxide particle-size means range from 60-70% of the corresponding oxalate means, and the uniformity (as measured by the FWHM) is about 50% better.

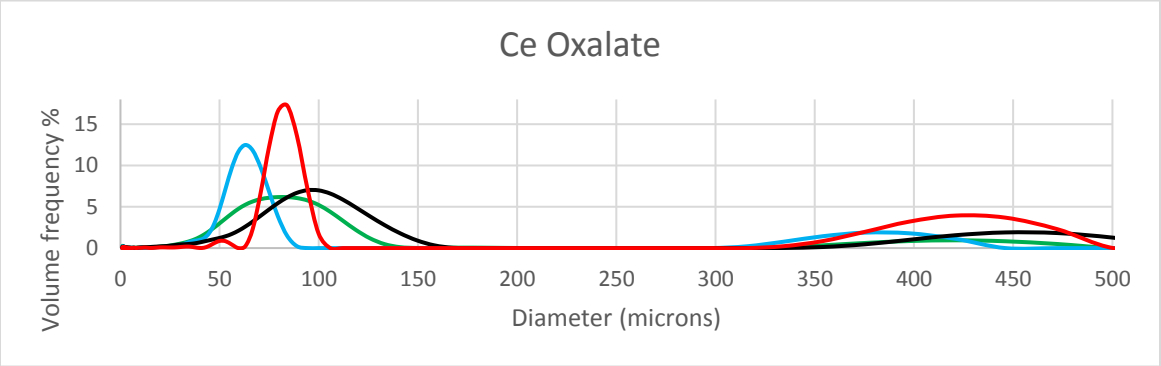

Ce Oxalate	Dose (sec)	Stirrer Rate	Mean (µm)	FWHM (µm)	
Ce-A	110	25%	82	63	direct strike
Ce-B	11	25%	63	24	direct strike
Ce-C	11	10%	97	60	direct strike
Ce-D	10 sec	25%	86	23	reverse strike

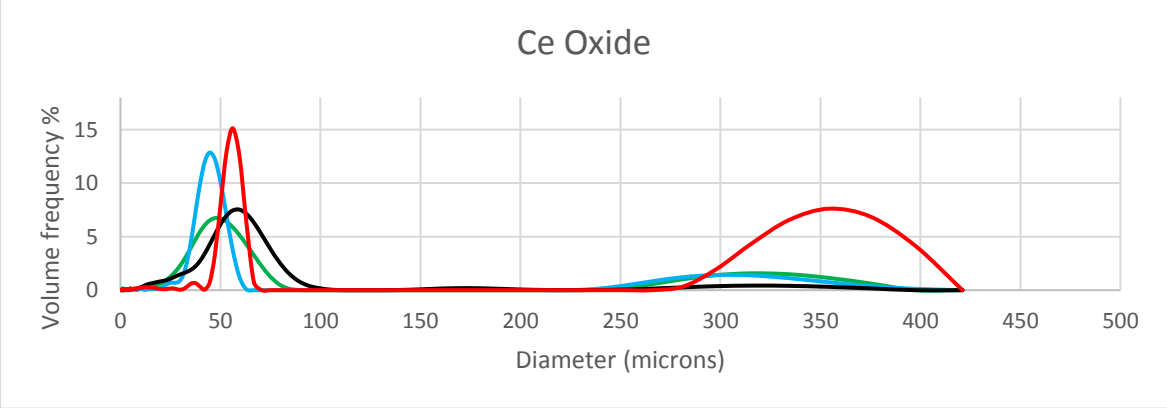

Ce Oxide	Dose (sec)	Stirrer Rate	Mean (µm)	FWHM (µm)	
Ce-A	110	25%	49	33	direct strike
Ce-B	11	25%	45	17	direct strike
Ce-C	11	10%	58	32	direct strike
Ce-D	10 sec	25%	56	12	reverse strike

In general, the particle-sizes determined in aqueous slurries agree with those seen in the SEM images. The following figure shows examples of a broad oxalate distribution and a narrow oxide distribution. The size of the larger particles in each image agree with the sizes for the upper wings of the slurry distributions.

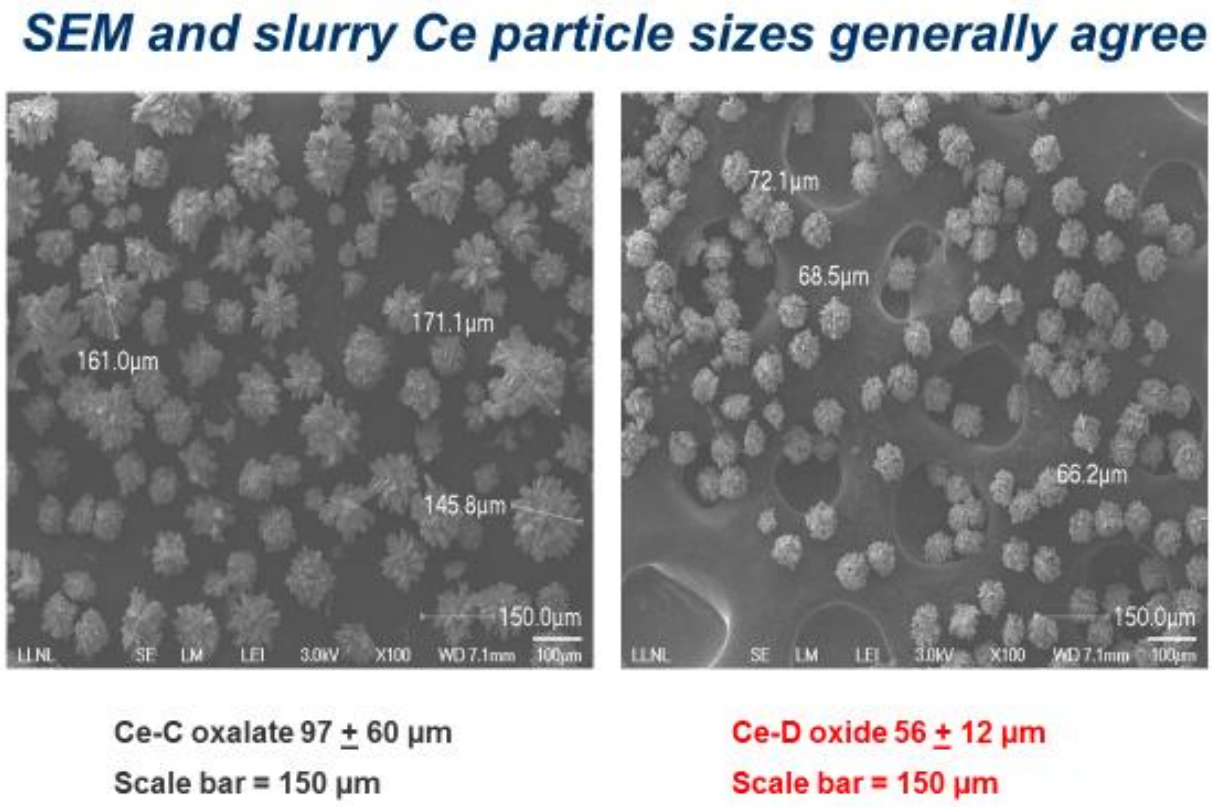

Minu et al (2016) have shown that single crystals of $Ce_2(Ox)_3 \cdot 10H_2O$ grow as hexagonal plates; however, clusters also form where the single crystals share edges.

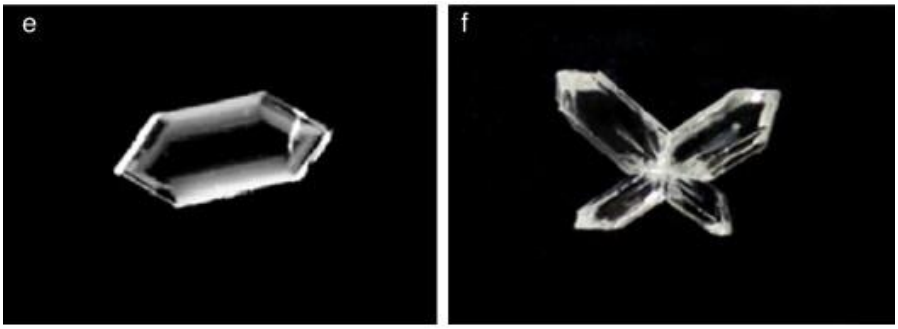

Minu et al, J. Mater. Res. Technol. 2016; **5(3)**: 268-274.

We show in the next figure this behavior for our Ce oxalates. However, we find many more clusters joined in the macroscopic particles than in the idealized case above.

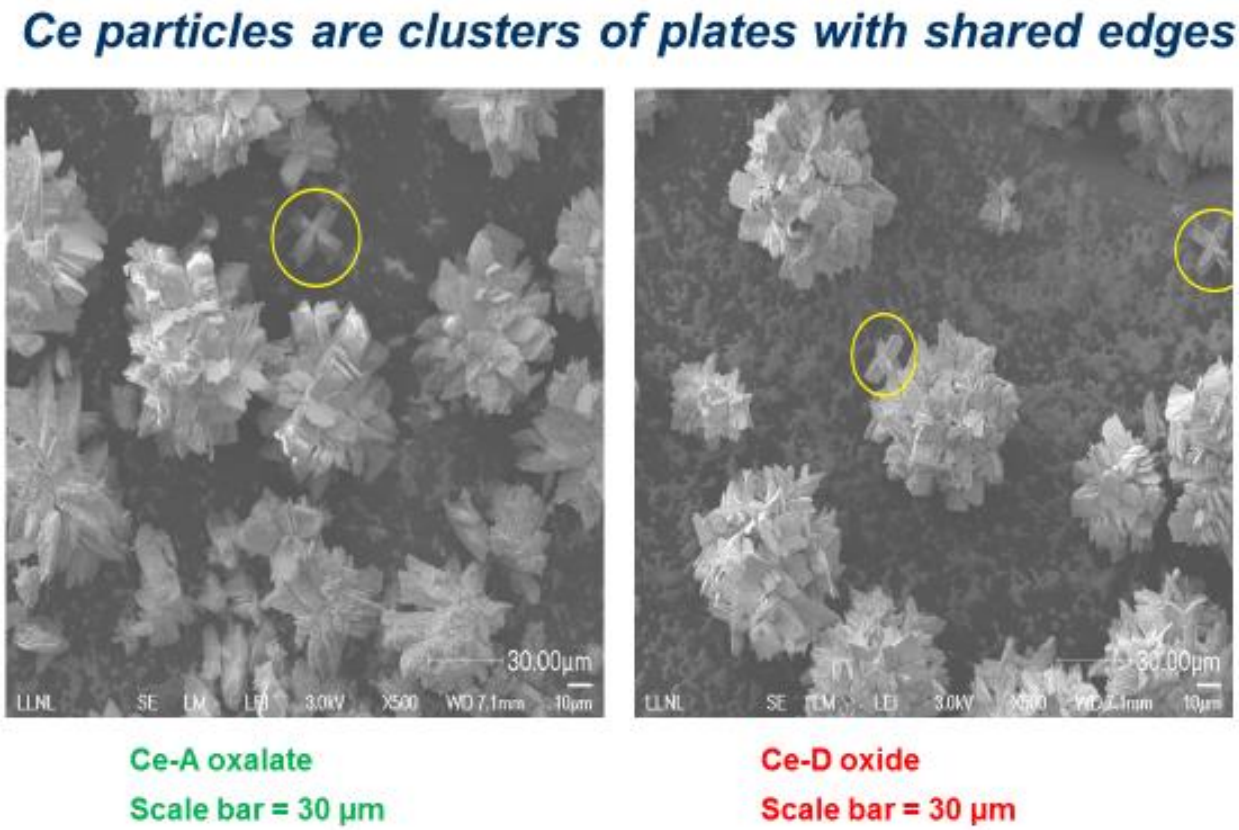

While searching for a forensic sign of different Ce oxalate growth conditions, we did find some particles grown under the poorest mixing conditions that looked different from the “normal” particles. Visually, it appears that the edges look more like dendrites or feathers than the smooth edge of a plate. This morphology is maintained in the calcined Ce oxide particle. However, we also see this feature in the other oxalates produced in this study, though not as dramatically as the example in the next figure. More work would be needed to test whether this is a useful diagnostic.

Ce particles can have feathery edges

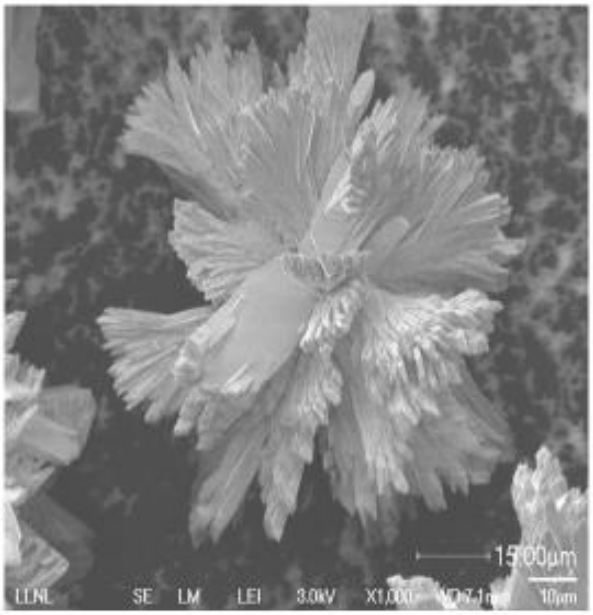

Ce-C oxalate
Scale bar = 15 µm

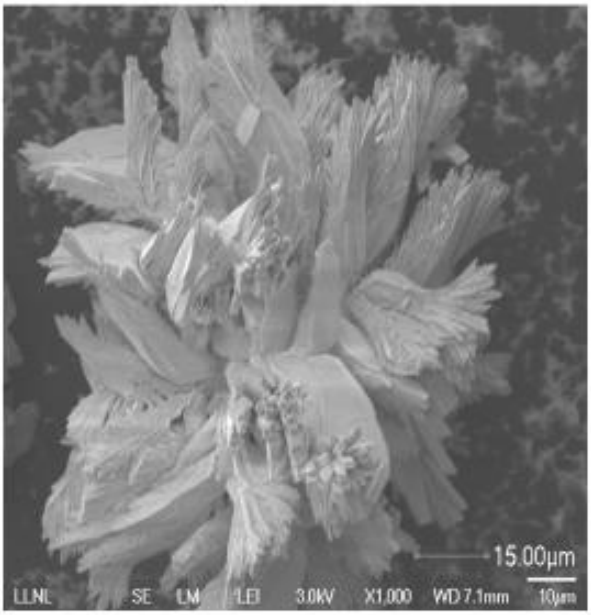

Ce-C oxide
Scale bar = 15 µm

Pu Results and Discussion

Like Ce, Pu oxalate particles grow as clusters of plates with shared edges.

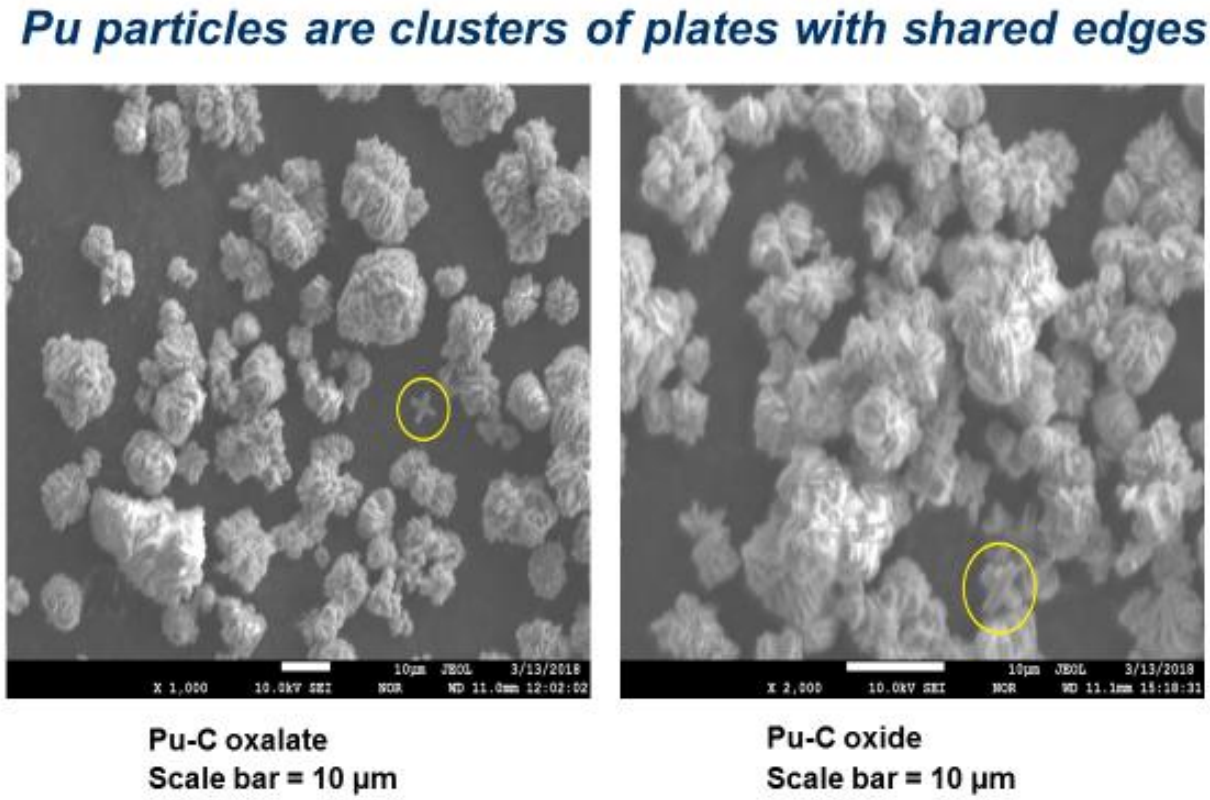

We observed a striking difference in packing densities for the Pu oxalates. The samples shown below have the same nominal weight (~1.7 ± 0.1 g), yet the best-mixed sample (Pu-A) is occupies one-third to one-half the volume as the others.

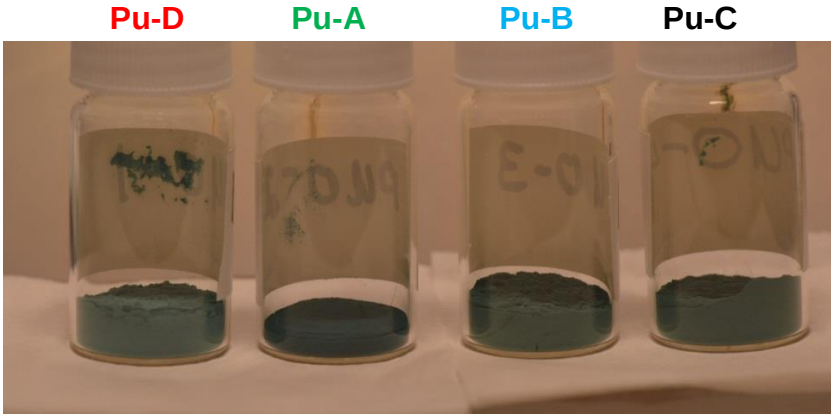

The Pu-A particles show a greater fraction of large particles compared to Pu-B, Pu-C, and Pu-D. More experiments are necessary to confirm the reproducibility of the possible size distribution differences.

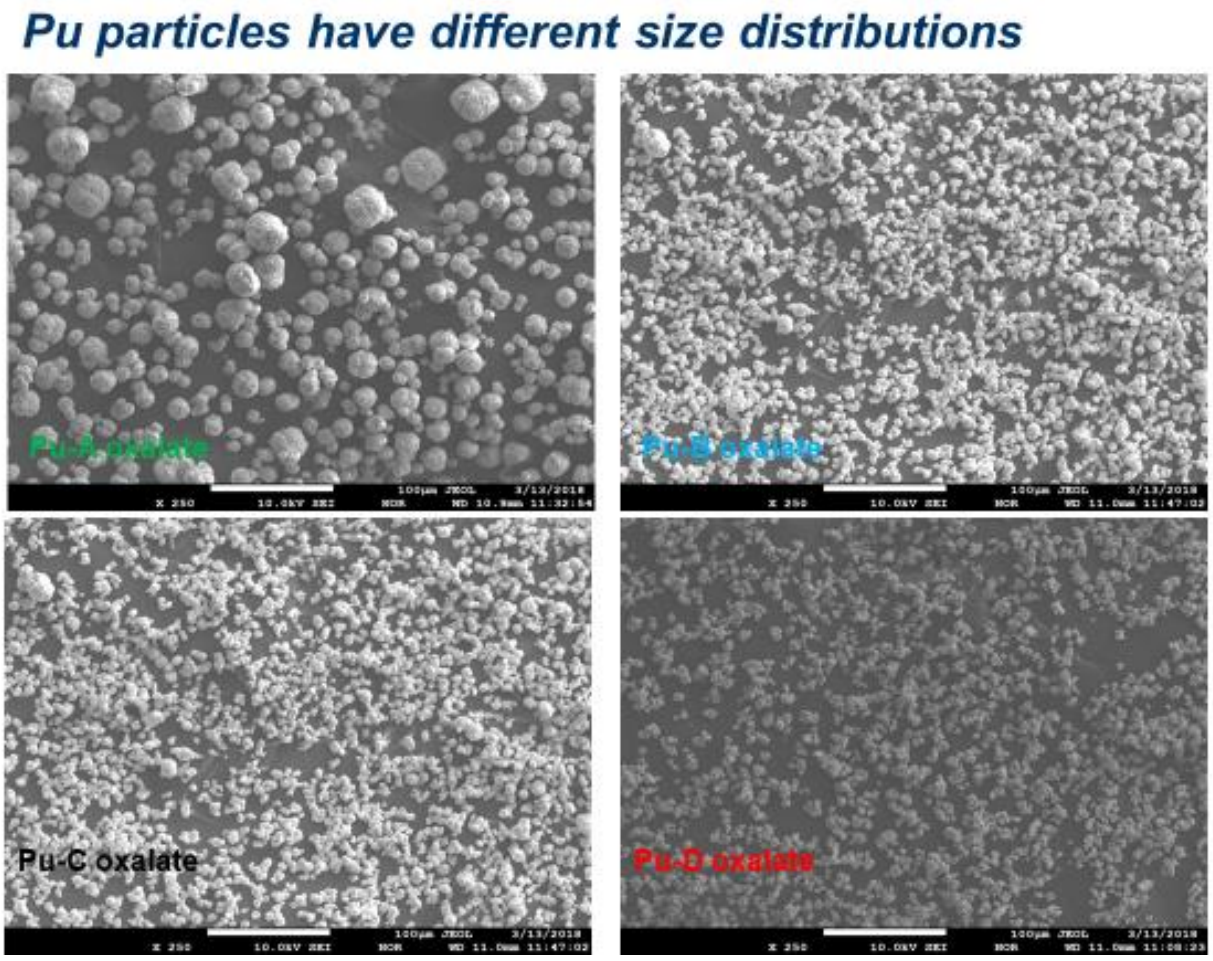

Scale bar = 100 μm **Scale bar = 100 μm**

Also, the Pu-A particles appear smoother and more spherical than the other Pu particles, although this might be an artifact due to the poorer visualization of the smaller particles for Pu-B, Pu-C, and Pu-D.

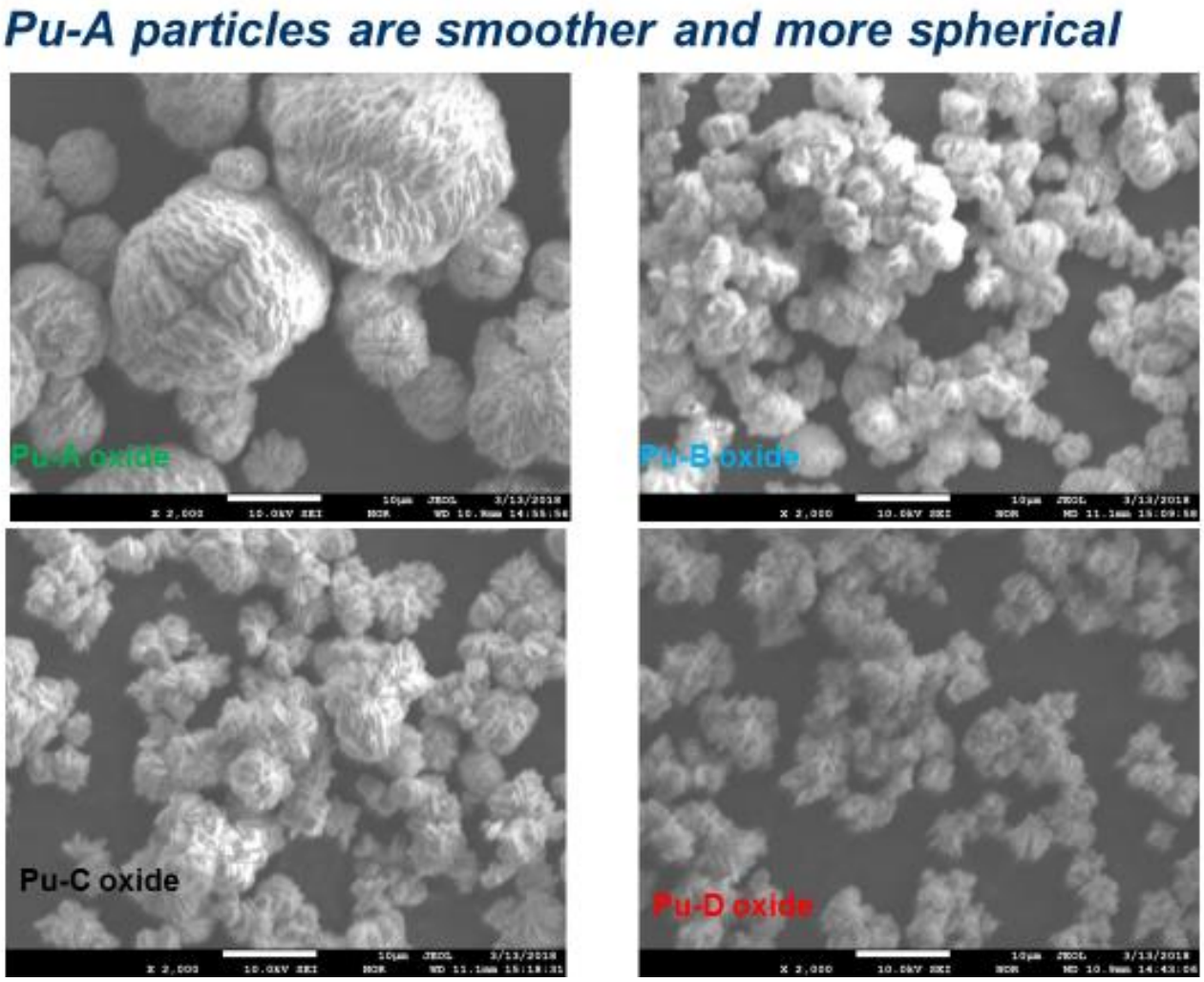

Scale bar = 10 μm **Scale bar = 10 μm**

The Pu particles produced are significantly smaller than the ones found for its Ce analogues. This suggests that more nucleation sites were created simultaneously in the Pu experiments than in the Ce ones, although the reason is unclear.